

**SIMULATION-BASED MODEL OF THERMAL ABLATION OF PROSTATE  
CANCER USING HIGH INTENSITY FOCUSED ULTRASOUND**

By

Abdulkareem Mas-ud Ayodeji

ID No.:40388

Supervised By:

Dr. Omololu Akin-Ojo



African University Of Science And Technology  
[www.aust.edu.ng](http://www.aust.edu.ng)  
P.M.B 681, Garki, Abuja F.C.T  
Nigeria.

December, 2014

**SIMULATION-BASED MODEL THERMAL ABLATION OF PROSTATE  
CANCER USING HIGH INTENSITY FOCUSED ULTRASOUND**

A Thesis

Presented To The Department Of

Theoretical Physics

African University Of Science And Technology

In Partial Fulfilment Of The Requirements

For The Degree Of

**MASTER OF SCIENCE**

By

**Abdulkareem Mas-ud Ayodeji**

Abuja, Nigeria

December, 2014

**SIMULATION-BASED MODEL THERMAL ABLATION OF PROSTATE  
CANCER USING HIGH INTENSITY FOCUSED ULTRASOUND**

By

Abdulkareem Mas-ud

A Thesis Approved By

The Theoretical Physics Department

Recommended: .....  
Supervisor: Dr. Omololu Akin-Ojo

.....  
Head, Department of Theoretical Physics

Approved: .....  
Chief Academic Officer

### **Abstract**

The use of High Intensity Focused Ultrasound (HIFU) in the medical treatment of cancer has attracted scientists and engineers with interest in achieving the most financially affordable but yet curative methods of curing different types of cancers. This present work considers a 2D modeling of the prostate gland without the environmental (neighbouring) tissues such as bladder, rectum, urethra and seminal vesicle. This model uses the nonlinear Westervelt equation since the propagation is in human tissue which is a nonlinear medium. Using a suitable application software (COMSOL) to solve the resulting equations, we predict the temperature distribution of the prostate when HIFU is applied. Our results are comparable to a similar work studied the acoustic streaming and convective cooling due to the use of HIFU.

---

## Acknowledgements

---

The first of all acknowledgement belongs to Almighty Allah. May His peace and blessing be upon the holy prophet Muhammad, his family, his faithful companions and those who follow his footstep till the day of judgement.

I am heartily grateful to my supervisor Dr. Omololu Akin-Ojo, who aside teaching and supervision has been a father to me in AUST, his guidance, and support from the beginning to the final stage of my M.Sc have turned me around.

My unquantifiable gratitude goes to BOVAS Group and Nelson Mandela Institute for sponsoring my M.Sc program, making me benefit from this world-class education. I acknowledge my siblings for the support; morally and in other ramifications. All the family members of Abdulkareem and Adeyemi are acknowledged in this project, thank you all.

My regards extends to my departmental colleagues in Physics as well as other students of African University of Science and Technology, Abuja. It is such a blessed experience knowing you all.

Above all, I am pleased to express my gratitude to my parents, having them is the most favourable gift from God.

---

## Dedication

---

I dedicate this project to the Glory of Almighty Allah, the creator and sustainer of everything. I also dedicate this work to my parents who have been with me since when I knew nothing till this stage of my life. I love you two.

<b>1</b>	<b>Introduction</b>	<b>4</b>
1.1	Previous Works on HIFU Application of Tumor ablation . . . . .	5
1.2	Acoustics . . . . .	5
1.3	Prostate Cancer . . . . .	6
<b>2</b>	<b>Governing Equations of Sound Propagation</b>	<b>7</b>
2.1	Introduction . . . . .	7
2.2	Euler’s Equation . . . . .	7
2.3	Navier-Stoke’s Equation . . . . .	10
2.4	The Entropy Equation . . . . .	11
2.5	General Fractional Wave Equation . . . . .	14
2.6	Pennes Bioheat Equation . . . . .	15
<b>3</b>	<b>Materials and Methods</b>	<b>18</b>
3.1	Methodology . . . . .	19
3.2	Boundary Condition . . . . .	21
3.3	PDE . . . . .	21
<b>4</b>	<b>Results and Discussion</b>	<b>22</b>
4.1	Conclusion . . . . .	23

Much attention has been paid to the uses of High Intensity Focused Ultrasound due to its profound and diverse applications in the medical industry. Among these applications are lithotripsy and thermotherapy. Lithotripsy involves the use of HIFU wave applied from an external source to physically destroy hardened tissue masses in the body. Thermotherapy, on the other hand, is the use of heat to cure diseases. Both thermotherapy and lithotripsy have a common advantage of being effective non-invasive treatment and enhanced healing process if properly used.

The present work will focus on the cure of prostate cancer with High Intensity Focused Ultrasound which is a class of thermotherapy. The source of the ultrasound is placed at the affected part and the propagation through the skin which is a complex media makes the technique not suitably described by the linear wave equation with integer order derivative[2]. The proper analysis of sound wave propagation and the attenuation through such complex media is better with the use of fractional derivative[3]

HIFU as a technique relies on the ability to model properly and accurately with the environmental boundary conditions, the propagation of sound waves through complex media such as body tissue. Hence, we shall use a nonlinear model due to the nonlinear material properties of the body tissue. There are many of such models among which are Kuznetsov–Zabolotskaya–Khokhlov (KZK)[4], Nonlinear Parabolic Equation (NPE) equation [5], and the Westervelt nonlinear wave equation. Most of the past study reviewed used the Westervelt equation to model the acoustic field generated by the HIFU source.

We shall use the fractional derivative form of the Westervelt equation in this study. The justification being that the fractional modified version according to the work of Fabrice and Sverre [6] gives us the ability to explain the propagation loss (both dispersion and attenuation) through complex media such as biological tissue. We shall see later that the Westervelt equation itself is derived from the Navier-Stokes' equation with some approximations using the “fractional form” of Euler's equation.

HIFU operates on two basic mechanisms. The thermal and mechanical mechanisms. While the



mechanical mechanism deals with the propagation of the generated wave through both air and the body tissue, the thermal mechanism governs the propagation of heat and the rapid elevation of the prostate temperature. The sound waves generated are collected at the focal point situated near the abdomen (Prostate gland is near this place). This causes the HIFU intensity to rise at the focal region to about several orders of magnitude  $100 - 10,000W/cm^2$  with peak compression pressures [7]. Focused ultrasound has its application in the clinical treatment of tumor and this can be categorized into two: Ultrasound Surgery (US) and hyperthermia. In the latter, the patient tumor is exposed to the ultrasound for a long period (about 10-60 mins) at low intensities at temperature about  $41^{\circ}C - 45^{\circ}C$  during the treatment.[9]. As a rule of thumb, the U.S Government has set a maximum thermal index as well as mechanical index, a dosage parameter indicating maximum temperature and time of exposure [10]. For this reason, most ultrasonic systems now come with displays with thermal index as well as mechanical index. The model in this study shows the simulation of curing a prostate cancer with HIFU. The result of this study is compared with studies mentioned in references [20] [12].

## 1.1 Previous Works on HIFU Application of Tumor ablation

The field of ultrasound surgery has experienced much research recently with the introduction of the application of clinical surgery. Solovchuk et al [11] found a significant effect of convective cooling and acoustic streaming in their imaged-based simulation of liver tumor ablation.

Prostate deformation after a clinical surgery was modelled by Simulation Open Framework Architecture (SOFA) [7] and it was found that the needle insertion simulation leads to displacement of about 0.14mm of the prostate with a peak error of 0.32mm. A similar work to this present study was done by Jafarian et al. [12] and revealed that the temperature rises with time during the first few minutes of the sonication. The findings in this research work agrees with the temperature elevation and the intensity of the ultrasound.

The mechanical deformation of the prostate gland would be difficult to observe if the mechanical properties are not well understood. Hwang et al in their article indicated that the prostate is hyperelastic and viscoelastic in nature[18]. In the case of the relationship of attenuation with angular frequency, the loss was modeled as proportional to  $\omega^{\gamma}$ , with  $\omega$  being the angular frequency and  $\gamma$  a non-integer. This therefore indicates that the attenuation of sound waves in complex media such as human tissue could be modeled using fractional derivative [6]

## 1.2 Acoustics

This is the branch of science that studies sound as it concerns the source, transmission and other properties of wave such as reflection, refraction, and diffraction. Originally, acoustics was the study of small pressure waves with frequencies in the range which is audible to human hearing. The scope of acoustic has since been extended to lower and higher frequencies[13]. Until recently, the nonlinear effects of acoustics was neglected. Among the literature on acoustics, the book of Pierce [14] has been very fundamental and useful.

### 1.3 Prostate Cancer

The prostate belongs to a group of exocrine glands of the male reproductive system and it is situated in the vicinity of the rectum, bladder, and urethra. An exocrine gland is one whose secretions end up outside the body such as in prostate and sweat glands. The prostate whose size is approximately that of a walnut helps the urethra to pass through from the bladder to the end of the penis. There are thousands of tiny glands in the prostate. These tiny glands produce fluids which form part of the semen and the fluid protects and nourishes the sperm. Also, the prostate gland helps in the control of urine flow through the urethra by contraction of the prostate muscle.

The cells in the prostate gland produce a special protein called Prostate Specific Antigen (PSA) which helps keep the semen in its liquid state. These protein antigens have the tendency of escaping into the blood stream and, because of this, the PSA level can be measured by checking the PSA content in the blood. A high PSA level most times indicates cancer or some kind of prostate condition.[15]

Prostate cancer is the development of abnormal growth of tissue in the prostate gland. This may lead to serious problems in a man ranging from the reproductive to the excretory system. In the reproductive system, prostate cancer may lead to infertility while in the excretory system it may cause the inability to control the flow of urine flowing through the urethra.

## 2.1 Introduction

In this chapter we shall discuss the basic equations of motions for viscous flows. The two most fundamental equations we shall mention are; i. Newton's equations of motion and ii. Equation of conservation of mass. Newton's equation in addition to the conservation of mass are useful in the derivation of the Euler equations which are sets of equations governing inviscid flow[22]. We shall use Euler's equation with the entropy equation to derive the Westervelt equation which governs the propagation of fluids in complex media, such as biological tissue putting into consideration the attenuation induced by this nonlinear medium[20]. The governing equations of computational fluid dynamics can be applied to both compressible as well as incompressible flow using an appropriate equation of state. This gives us the justification to apply the equations in describing the propagation of propagation of sound waves both in air and in the tissue.

We start by briefly discussing Euler's equations from Newton's second equation of motion and proceed to introduce the fractional form of Navier-Stoke's equation. Also the Entropy equation is derived using Fourier's law as a constitutive relation. By combining the derived Navier-Stokes and Entropy equations, we get a wave equation which, by following some approximations leads to a generalization of the Westervelt equation.

## 2.2 Euler's Equation

From Newton's second law of motion which describes the conservation of linear momentum,

$$F = \frac{Dp}{Dt} \quad (2.1)$$

where  $F$  is the resultant force acting on the fluid mass and  $p$  is the linear momentum defined as

$$P = \int_{sys} V dm \quad (2.2)$$

Where  $V$  is the control volume and the operator  $\frac{D}{Dt}$  is the material derivative defined by

$$\frac{D}{Dt} = \frac{\partial}{\partial t} + u \frac{\partial}{\partial x} + v \frac{\partial}{\partial y} + w \frac{\partial}{\partial z} \quad (2.3)$$

In the above,  $u$ ,  $v$ , and  $w$  are the velocity components in the  $x$ ,  $y$ , and  $z$  directions respectively and  $t$  is the time (see reference [1], for example). We can apply equation 2.1 to a differential system consisting of a mass  $\delta m$  to give

$$\delta F = \frac{D}{Dt} v \delta m \quad (2.4)$$

For a non viscous fluid,  $\delta m$  can be treated as a constant, so that

$$\delta F = \delta m \frac{Dv}{Dt} \quad (2.5)$$

where  $\frac{Dv}{Dt}$  is the acceleration of the body mass. The equation above therefore leads to

$$\delta F = a \delta m \quad (2.6)$$

In component form, we can write a set of equations as follows.

$\delta F_x = a_x \delta m$ ,  $\delta F_y = a_y \delta m$ ,  $\delta F_z = a_z \delta m$ , and using the equation 2.3 for the acceleration, we obtain

$$\begin{aligned} a_x &= \frac{\partial u}{\partial t} + u \frac{\partial u}{\partial x} + v \frac{\partial u}{\partial y} + w \frac{\partial u}{\partial z} \\ a_y &= \frac{\partial v}{\partial t} + u \frac{\partial v}{\partial x} + v \frac{\partial v}{\partial y} + w \frac{\partial v}{\partial z} \\ a_z &= \frac{\partial w}{\partial t} + u \frac{\partial w}{\partial x} + v \frac{\partial w}{\partial y} + w \frac{\partial w}{\partial z} \end{aligned} \quad (2.7)$$

where  $u$ ,  $v$ , and  $w$  are the  $x$ ,  $y$ , and  $z$  components of the velocity respectively.

Consider a differential element of a fluid. The forces acting on it can be categorized into two: surface forces and body force, if the only body force acting on the fluid is its weight then the body force is given by

$$\delta \mathbf{F}_b = \mathbf{g} \delta m \quad (2.8)$$

where in component form,  $\delta F_{bx} = g_x \delta m$ ,  $\delta F_{by} = g_y \delta m$ , and  $\delta F_{bz} = g_z \delta m$ , with  $g_x$ ,  $g_y$ , and  $g_z$  representing  $x$ ,  $y$ , and  $z$  components of acceleration due to gravity respectively.

To account for the surface forces, we consider figure ?? which shows an elemental volume of fluid across the area ABCD as shown, where,  $\sigma_{xx}$  is the normal stress in the  $x$ -direction with a corresponding force of  $\delta F_{xx} = \partial \sigma_{xx} \delta y \delta z$ ,  $\sigma_{yx}$  is the shear stress in the  $x - y$  plane with a corresponding force of  $\delta F_{yx} = \partial \sigma_{yx} \delta x \delta z$ , and  $\sigma_{zx}$  is the shear stress in the  $x - z$  plane with its

corresponding force of  $\delta F_{zx} = \partial\sigma_{zx}\delta x\delta y$

The total surface force in the x-direction  $\delta F_{sx}$  can thus be written as

$$\delta F_{sx} = \left( \frac{\partial\sigma_{xx}}{\partial x} + \frac{\partial\sigma_{yx}}{\partial y} + \frac{\partial\sigma_{zx}}{\partial z} \right) \delta x\delta y\delta z \quad (2.9)$$

and similarly in the  $x$  and  $y$  directions

$$\delta F_{sy} = \left( \frac{\partial\sigma_{xy}}{\partial x} + \frac{\partial\sigma_{yy}}{\partial y} + \frac{\partial\sigma_{zy}}{\partial z} \right) \delta x\delta y\delta z$$

$$\delta F_{sz} = \left( \frac{\partial\sigma_{xz}}{\partial x} + \frac{\partial\sigma_{yz}}{\partial y} + \frac{\partial\sigma_{zz}}{\partial z} \right) \delta x\delta y\delta z$$

The total force in the x-direction is the sum of the resultant surface in the x-direction and the x-component of body force given as

$$\delta F_x = \delta F_{sx} + \delta F_{bx} \quad (2.10)$$

By using the expression for the body force in equation 2.10

$$\delta F_x = \delta F_{sx} + \delta mg_x \quad (2.11)$$

we can express the elemental mass in terms of the density as  $\delta m = \rho\delta x\delta y\delta z$ , so that equation 2.11 becomes

$$\delta F_x = \delta F_{sx} + g_x\rho\delta x\delta y\delta z \quad (2.12)$$

From Newton's second law, we can write

$$\delta F_x = a_x\rho\delta x\delta y\delta z \quad (2.13)$$

Using equation 2.7 in equation 2.13, we obtain

$$\delta F_x = \rho \left( \frac{\partial u}{\partial t} + u\frac{\partial u}{\partial x} + v\frac{\partial u}{\partial y} + w\frac{\partial u}{\partial z} \right) \delta x\delta y\delta z \quad (2.14)$$

Substituting equation 2.9 and 2.14 into 2.12, gives us the total force in the x-direction as follows

$$\rho \left( \frac{\partial u}{\partial t} + u\frac{\partial u}{\partial x} + v\frac{\partial u}{\partial y} + w\frac{\partial u}{\partial z} \right) = \left( \frac{\partial\sigma_{xx}}{\partial x} + \frac{\partial\sigma_{yx}}{\partial y} + \frac{\partial\sigma_{zx}}{\partial z} \right) + \rho g_x \quad (2.15)$$

and for the corresponding forces in the  $y$  and  $z$  directions

$$\rho \left( \frac{\partial v}{\partial t} + u\frac{\partial v}{\partial x} + v\frac{\partial v}{\partial y} + w\frac{\partial v}{\partial z} \right) = \left( \frac{\partial\sigma_{xy}}{\partial x} + \frac{\partial\sigma_{yy}}{\partial y} + \frac{\partial\sigma_{zy}}{\partial z} \right) + \rho g_y$$

$$\rho \left( \frac{\partial w}{\partial t} + u\frac{\partial w}{\partial x} + v\frac{\partial w}{\partial y} + w\frac{\partial w}{\partial z} \right) = \left( \frac{\partial\sigma_{xz}}{\partial x} + \frac{\partial\sigma_{yz}}{\partial y} + \frac{\partial\sigma_{zz}}{\partial z} \right) + \rho g_z$$

The three expressions in equation 2.15 can be written in short form as

$$\rho \left( \frac{\partial v_i}{\partial t} + v_k \frac{\partial v_i}{\partial x_k} \right) = - \frac{\partial p}{\partial x_i} \quad (2.16)$$

Equation 2.16 is the Euler's equation.

## 2.3 Navier-Stoke's Equation

The stress in a fluid can be split into two components: the one that acts normal to the surface of the fluid and the component due to viscosity. For a static or frictionless fluid, the normal stresses are equal in all directions which indicates that the stress tensor is isotropic or symmetric. Any isotropic second-order tensor must be proportional to the Kronecker delta [1] as given below

$$\sigma_{ik} = -p\delta_{ik} \quad (2.17)$$

To determine the stress due to the flow of viscous fluid, we consider the fluid as isotropic and that the properties of the fluid are described by scalar quantities only such that we can define a stress tensor which contains the scalar properties of the fluid and linear combinations of the derivatives ( $\frac{\partial v_i}{\partial x_k}$ ) as described in [8] for a Newtonian fluid. Therefore we can express the stress tensor as follows

$$\sigma'_{ik} = \eta \left[ \frac{\partial v_i}{\partial x_k} + \frac{\partial v_k}{\partial x_i} - \frac{2}{3} \delta_{ik} \frac{\partial v_l}{\partial x_l} \right] + \zeta \delta_{ik} \frac{\partial v_l}{\partial x_l} \quad (2.18)$$

where  $\eta$  and  $\zeta$  are both scalar quantities describing the properties of the fluid and independent of the fluid velocity. They are called coefficients of viscosity [8]. In the equation above, summation is taken over repeated indices.

By adding the rate of change of the stress tensor with the position to the right hand side of equation 2.4 we get

$$\rho \left( \frac{\partial v_i}{\partial t} + v_k \frac{\partial v_i}{\partial x_k} \right) = -\frac{\partial p}{\partial x_i} + \frac{\partial \sigma'_{ik}}{\partial x_k} \quad (2.19)$$

The derivative of the stress tensor in equation 2.10 with respect to  $x_k$  is given by

$$\frac{\partial \sigma'}{\partial x_k} = \eta \frac{\partial}{\partial x_k} \left[ \frac{\partial v_i}{\partial x_k} + \frac{\partial v_k}{\partial x_i} - \frac{2}{3} \delta_{ik} \frac{\partial v_l}{\partial x_l} \right] + \zeta \delta_{ik} \frac{\partial}{\partial x_k} \frac{\partial v_l}{\partial x_l} \quad (2.20)$$

$$\frac{\partial \sigma'}{\partial x_k} = \eta \left[ \frac{\partial^2 v_i}{\partial x_k \partial x_k} + \frac{\partial^2 v_k}{\partial x_k \partial x_i} - \frac{2}{3} \delta_{ik} \frac{\partial^2 v_l}{\partial x_k \partial x_l} \right] + \zeta \delta_{ik} \frac{\partial^2 v_l}{\partial x_k \partial x_l} \quad (2.21)$$

By way of simplification, we may add and subtract  $\frac{1}{3} \delta_{ik} \frac{\partial^2 v_l}{\partial x_k \partial x_l}$  to the terms inside the square bracket and regroup to give

$$\frac{\partial \sigma'}{\partial x_k} = \eta \left[ \frac{\partial^2 v_i}{\partial x_k \partial x_k} + \frac{\partial^2 v_k}{\partial x_k \partial x_i} - \delta_{ik} \frac{\partial^2 v_l}{\partial x_k \partial x_l} \right] + \left( \zeta + \frac{\eta}{3} \right) \delta_{ik} \frac{\partial^2 v_l}{\partial x_k \partial x_l} \quad (2.22)$$

but note that the Einstein Summation Convention is employed in  $\frac{\partial v_l}{\partial x_l}$ . This means that

$$\frac{\partial v_l}{\partial x_l} = \frac{\partial v_1}{\partial x_1} + \frac{\partial v_2}{\partial x_2} + \frac{\partial v_3}{\partial x_3} \quad (2.23)$$

And since the velocity is continuous, the expression after evaluating the kronecker delta  $\delta_{ik}$  becomes

$$\frac{\partial \sigma'}{\partial x_k} = \eta \frac{\partial^2 v_i}{\partial x_k \partial x_k} + \left( \zeta + \frac{\eta}{3} \right) \frac{\partial^2 v_l}{\partial x_i \partial x_l} \quad (2.24)$$

where from the Einstein Summation Convention,

$$\frac{\partial v_l}{\partial x_l} = \frac{\partial v_x}{\partial x} + \frac{\partial v_y}{\partial y} + \frac{\partial v_z}{\partial z} = \nabla \cdot \mathbf{v} \quad (2.25)$$

Using equation 2.25 in 2.19, we obtain

$$\rho \left[ \frac{\partial \mathbf{v}}{\partial t} + (\mathbf{v} \cdot \nabla) \mathbf{v} \right] = -\nabla P + \eta \nabla^2 \mathbf{v} + \left( \zeta + \frac{\eta}{3} \right) \nabla (\nabla \cdot \mathbf{v}) \quad (2.26)$$

By re-writing equation 2.26 in fractional derivative form, we get

$$\rho \left[ \frac{\partial \mathbf{v}}{\partial t} + (\mathbf{v} \cdot \nabla) \mathbf{v} \right] = -\nabla P + \tau^{\gamma-1} \nabla^2 \mathbf{v} + \tau^{\gamma-1} \left( \zeta + \frac{\eta}{3} \right) |^{1-\gamma} [\nabla (\nabla \cdot \mathbf{v})] \quad (2.27)$$

where  $|^{1-\gamma}$  is the fractional integral of order  $1 - \gamma$ .

Equation 2.27 is the fractional integral generalization of Navier-Stoke's equation with the bold-face letters designating vector quantities. Simplifying equation 2.27 for thermoviscous fluid we obtain the fracional form of Euler's equation, the mathematical steps are in [22] for verification. For thermoviscous fluid

$$\rho_0 \frac{\partial \mathbf{v}}{\partial t} = -\nabla P' + \left( \zeta + \frac{\eta}{3} \right) |^{1-\gamma} [\nabla^2 \mathbf{v}] - \frac{\rho}{2} \nabla^2 \mathbf{v} - \rho' \frac{\partial \mathbf{v}}{\partial t} \quad (2.28)$$

where  $\rho' = \rho - \rho_0$  and  $P' = P - P_0$  represent the dynamic density and pressure which describe the perturbation of the fluid from equilibrium positions.

## 2.4 The Entropy Equation

Entropy is commonly understood as a measure of disorder, it is therefore necessary to derive the entropy expression used in this modeling since it describes the thermodynamics of the system. The constitutive equation used in deriving the entropy is the Fourier law given by

$$\mathbf{q} = -k \nabla T$$

In 1958, Cattaneo and Vernotte [16][17] modified the equation above by adding a term on the left handside of the existing Fourier law as given below

$$\mathbf{q} + \tau_{cv} \frac{\partial \mathbf{q}}{\partial t} = -k \nabla T \quad (2.29)$$

where  $\tau_{cv}$  is a relaxation-time constant,  $\mathbf{q}$  is the heat flux,  $k$  is the thermal conductivity and  $T$  is the absolute temperature.

In 1968, Gurtin and Pipkin [19] introduced a more general time-non-local relationship between the heat flux transfer and temperature gradient. The Gurtin & Pipkin expression is

$$\mathbf{q}(t) = \int_0^\infty k(\tau) \nabla T(t - \tau) d\tau \quad (2.30)$$

Following the work of Fabrice and Sverre [20]

$$q(t) = - \int_0^t k(t-\tau) \nabla T(\tau) d\tau \quad (2.31)$$

considering that at initial time  $t < 0$ ,  $\nabla T = 0$  The relaxation function in accordance with Chandra Sekharaiah [21] can be related to a time-non-local kernel defined as

$$k(t-\tau) = \frac{\kappa}{\Gamma(\alpha-1)} (t-\tau)^{\alpha-2} \quad (2.32)$$

where  $\kappa$  is a positive constant. Substituting equation 2.32 into 2.31

$$q(t) = - \int_0^t \frac{\kappa}{\Gamma(\alpha-1)} (t-\tau)^{\alpha-2} \nabla T(\tau) d\tau \quad (2.33)$$

but  $\frac{\kappa}{\Gamma(\alpha-1)}$  is a constant of integration. If we substitute  $\alpha = \alpha + 1$

$$q(t) = - \frac{\kappa}{\Gamma(\alpha)} \int_0^t (t-\tau)^{\alpha-1} \nabla T(\tau) d\tau \quad (2.34)$$

Equation 2.34 can be compared to the definition of the fractional integral as follow [20]

$$|^\alpha [f(t)] = \frac{1}{\Gamma(\alpha)} \int_0^t (t-\tau)^{\alpha-1} f(\tau) d\tau \quad (2.35)$$

Using equation 2.35 in 2.33, we may therefore write equation 2.33 as

$$q(t) = -\kappa |^\alpha [\nabla T(t)] \quad (2.36)$$

Equation 2.36 is the modified Fourier constitutive relation in fractional integral form. A relationship can be established between equation 2.36 above and the thermal energy equation given below.

$$\nabla q(t) = -\rho C_p \frac{\partial T}{\partial t} \quad (2.37)$$

By taking the gradient of equation 2.36 in one dimension, we obtain

$$\frac{dq}{dx} = -\kappa \frac{d}{dx} |^\alpha [\nabla T(t)]$$

and multiplying both sides by  $\frac{dx}{dt}$  and using continuity property of  $q$ , we get

$$v_x \frac{dq}{dx} = -\kappa \frac{d}{dt} |^\alpha [\nabla T(t)] \quad (2.38)$$

Using the relationship between integral and derivative fractional operatives given in equation 2.38 below,

$$\frac{d}{dt} |^\alpha = \begin{cases} \frac{d^{\gamma-\alpha}}{dt^{\gamma-\alpha}} & 0 < \alpha < \gamma \\ |^{\alpha-\gamma} & 0 < \gamma < \alpha \end{cases} \quad (2.39)$$



but

$$\frac{d}{dt} |\alpha-1| [\nabla T(t)] = |\alpha-2| [\nabla T(t)] \quad (2.40)$$

Using equation 2.39 in 2.38

$$v_x \frac{dq}{dx} = -\kappa |\alpha-2| [\nabla T(t)] \quad (2.41)$$

If we consider equation 2.37 in one dimension, multiply both sides by  $v_x$  and compare with equation 2.41

$$-\rho C_p \frac{\partial T}{\partial t} = -\kappa |\alpha-2| [\nabla T(t)] \quad (2.42)$$

Differentiating both sides  $(\alpha - 1)$  times considering  $v_x$  as a constant of time

$$\rho C_p v_x \frac{d^{\alpha-1}}{dt^{\alpha-1}} \frac{\partial T}{\partial t} = -\kappa \frac{d^{\alpha-1}}{dt^{\alpha-1}} |\alpha-2| \left[ \frac{dT}{dx} \right] \quad (2.43)$$

Applying the definition of fractional integral to equation 2.43

$$\rho C_p v_x \frac{d^\alpha T}{dt^\alpha} = \kappa \frac{d}{dt} \left( \frac{dT}{dx} \right) \quad (2.44)$$

and using  $\frac{d}{dt} = \frac{dx}{dt} \frac{d}{dx}$  thereby cancelling  $v_x$  from both sides to give

$$\begin{aligned} \rho C_p \frac{d^\alpha T}{dt^\alpha} &= \kappa \frac{d^2 T}{dx^2} \\ \frac{1}{D} \frac{d^\alpha T}{dt^\alpha} &= \frac{d^2 T}{dx^2} \end{aligned} \quad (2.45)$$

Where D is the diffusivity defined by  $D = \frac{\kappa}{\rho C_p}$  Expressing equation 2.45 back in three dimension

$$\frac{1}{D} \frac{d^\alpha T}{dt^\alpha} = \nabla^2 T \quad (2.46)$$

The dimension of D and  $\kappa$  can be derived from equations 2.46 and 2.36 respectively using dimensional analysis as done by Fabrice and Sverre in equation 21 of [6]

$$\nabla^2 T = \frac{\tau_{th}^{\alpha-2}}{C_0^2} \frac{\partial^\alpha T}{\partial t^\alpha} \quad (2.47)$$

Comparing equation 2.47 with equation 33 of [22], we obtain

$$\rho_0 T_0 \frac{\partial s}{\partial t} = \kappa \nabla^2 T \quad (2.48)$$

2.48 From the two equations above,

$$\frac{\rho_0 T_0}{\kappa} \frac{\partial s}{\partial t} = \nabla^2 T$$

and

$$\frac{\rho_0 T_0}{\kappa} \frac{\partial s}{\partial t} = \frac{\tau_{th}^{\alpha-2}}{c_0^2} \frac{\partial^\alpha T}{\partial t^\alpha} \quad (2.49)$$

Where  $\kappa$  is the thermal conductivity,  $T_0$  is the equilibrium temperature,  $\rho_0$  the equilibrium density,  $C_0$  the speed of sound in the medium and  $\tau_{th}$  is the thermal relaxation time of the medium.

## 2.5 General Fractional Wave Equation

With the help of the functional Euler and entropy equations found in the section above, we shall obtain a wave equation with fractional derivatives. From the approximation made by Hamilton and Morfey [22], the fractional Euler equation in section 2.3 above is simplified as follows:

$$\rho_0 \frac{\partial \mathbf{v}}{\partial t} = -\nabla P - \frac{\tau^{\gamma-1}}{\rho_0 C_0^2} \left( \zeta + \frac{4}{3} \eta \right) \frac{\partial \gamma}{\partial t} \nabla P - \nabla L \quad (2.50)$$

Where L is the second-order Lagrangian Density defined as

$$L = \frac{1}{2} \rho_0 v^2 - \frac{P^2}{2 \rho_0 C_0^2} \quad (2.51)$$

The prime notation has been dropped from equation 2.28 but  $p$  still represent the dynamic pressure from this point [20] and by making an approximation made in Ref [22], we obtain a continuity equation [22]

$$\frac{\partial p'}{\partial t} + \rho_0 \nabla \cdot \mathbf{v} = \frac{1}{\rho_0 c_0^4} \frac{\partial p^2}{\partial t} + \frac{1}{c_0^2} \frac{\partial L}{\partial t} \quad (2.52)$$

The equation above is one of the contributors of the nonlinear term in the Westervelt equation. Following the same step as [22] we will also introduce the equation of state as a Taylor series of the pressure  $P(\rho, s)$  about the equilibrium state  $(\rho_0, s_0)$  and neglect other terms of order three and above:

$$p = c_0^2 \rho' + \frac{c_0^2 \mathbf{B}}{\rho_0 2A} \rho'^2 + \left( \frac{\partial P}{\partial s} \right)_{\rho,0} s' \quad (2.53)$$

where  $\frac{B}{A}$  is the medium parameter of nonlinearity and  $s' = s - s_0$  is the dynamic entropy. This equation is also a nonlinear equation and it is the second source nonlinearity in the wave equation. Introducing  $T' = T - T_0$  and  $s = s' + s_0$  into equation 2.49:

$$\frac{\rho_0 T_0}{\kappa} \frac{\partial (s' + s_0)}{\partial t} = \frac{\tau_{th}^{\alpha-2}}{c_0^2} \frac{\partial^\alpha (T' + T_0)}{\partial t^\alpha} \quad (2.54)$$

for a constant  $T_0$  and  $s_0$ ,  $\frac{\partial (s' + s_0)}{\partial t} = \frac{\partial s'}{\partial t}$  and  $\frac{\partial^\alpha (T' + T_0)}{\partial t^\alpha} = \frac{\partial^\alpha T'}{\partial t^\alpha}$  Using these equations and integrating equation 2.49

$$\frac{\rho_0 T_0}{\kappa} s' = \frac{\tau_{th}^{\alpha-2}}{c_0^2} \frac{\partial^{\alpha-1} T'}{\partial t^{\alpha-1}}$$

so that

$$s' = \frac{\tau_{th}^{\alpha-2}}{c_0^2 \rho_0 T_0} \frac{\partial^{\alpha-1} T'}{\partial t^{\alpha-1}} \quad (2.55)$$

Substituting equation 2.54 in 2.53 so that we can eliminate  $s'$  in favour of  $T'$

$$p = c_0^2 \rho' + \frac{c_0^2 \mathbf{B}}{\rho_0 2A} \rho'^2 + \left( \frac{\partial P}{\partial s} \right)_{\rho,0} \frac{\tau_{th}^{\alpha-2}}{c_0^2 \rho_0 T_0} \frac{\partial^{\alpha-1} T'}{\partial t^{\alpha-1}} \quad (2.56)$$

If we follow the steps described in Hamilton & Morfey (see Ref.[22] for a detailed description), we arrive at the following equation:

$$\rho' = \frac{p}{c_0^2} + \frac{1}{\rho_0 c_0^4} \frac{B}{2A} p^2 - \frac{\kappa \tau_{th}^{\alpha-2}}{c_0^4 \rho_0} \left( \frac{1}{c_v} - \frac{1}{c_p} \right) \frac{\partial^{\alpha-1} p}{\partial t^{\alpha-1}} \quad (2.57)$$

where  $c_v$  and  $c_p$  are the heat capacity per unit mass at constant volume and constant pressure respectively. Subtracting the time derivative of equation 2.52 from the divergence of equation 2.50 as described by [20], we get

$$\left( \nabla^2 - \frac{1}{c_0^2} \frac{\partial^2}{\partial t^2} \right) p + \frac{\tau^{\gamma-1}}{\rho_0 c_0^2} \left( \zeta + \frac{4}{3} \eta \right) \frac{\partial^\gamma}{\partial t^\gamma} \nabla^2 p + \frac{\kappa \tau_{th}^{\alpha-2}}{c_0^4 \rho_0} \left( \frac{1}{c_v} - \frac{1}{c_p} \right) \frac{\partial^{\alpha+1} p}{\partial t^{\alpha+1}} = -\frac{\beta}{\rho_0 c_0^4} \frac{\partial^2 p^2}{\partial t^2} - \left( \nabla^2 + \frac{1}{c_0^2} \frac{\partial^2}{\partial t^2} \right) L \quad (2.58)$$

where  $\beta = 1 + \frac{B}{2A}$  is the coefficient of nonlinearity and other terms have their usual meanings. Equation 2.58 can be written in a short hand form and is interpreted as Westervelt equation, as given below

$$\left( \nabla^2 - \frac{1}{c_0^2} \frac{\partial^2}{\partial t^2} \right) p + L_v \frac{\partial^\gamma}{\partial t^\gamma} \nabla^2 p - \frac{L_t}{c_0^2} \frac{\partial^{\alpha+1} p}{\partial t^{\alpha+1}} = -\frac{\beta}{\rho_0 c_0^4} \frac{\partial^2 p^2}{\partial t^2} \quad (2.59)$$

where

$$L_v = \frac{\tau^{\gamma-1}}{\rho_0 c_0^2} \left( \zeta + \frac{4}{3} \eta \right)$$

$$L_t = \frac{\kappa \tau_{th}^{\alpha-2}}{c_0^2 \rho_0} \left( \frac{1}{c_v} - \frac{1}{c_p} \right)$$

for  $L_v > L_t$

The first term on the left hand side of equation 2.59 characterizes diffraction. The second and third terms characterize the attenuation coming from the fractional Euler's equation and the Entropy equation respectively.[20] The term on the right hand side is the factor of nonlinearity characterizing the attenuation arising from the complex medium and it comes from the continuity equation and the equation of state.

For us to get a fractional form of the Westervelt equation with a non-integer frequency power attenuation law, we set  $\gamma = y - 1$  where  $1 > y \leq 2$ .

From the wave equation,  $\nabla^2 p$  is approximated as  $\frac{1}{c_0^2} \frac{\partial^2 p}{\partial t^2}$ .

Equation 2.59 leads to the Westervelt equation.

$$\left( \nabla^2 - \frac{1}{c_0^2} \frac{\partial^2}{\partial t^2} \right) p + \frac{\delta}{c_0^4} \frac{\partial^3 p}{\partial t^3} = -\frac{\beta}{\rho_0 c_0^4} \frac{\partial^2 p^2}{\partial t^2} \quad (2.60)$$

## 2.6 Pennes Bioheat Equation

Among all mathematical models that have been developed over many years to describe heat transfer within living biological tissue, the most widely used bioheat model was Pennes Bioheat model, proposed by Pennes in 1948 and has been adopted into analysis of hyperthermia in cancer treatment. The assumptions made in developing Pennes Bioheat equation are listed below:

1. All pre-arteriole and post-venule heat transfer between blood and tissue is neglected.
2. The flow of blood in the small capillaries is assumed to be isotropic. This neglects the effect of blood flow directionality.
3. Larger blood vessels in the vicinity of capillary beds play no role in the energy exchange between tissue and capillary blood. Thus the Pennes model does not consider the local vascular geometry.
4. Blood is assumed to reach the arterioles supplying the capillary beds at the body core temperature. It instantaneously exchanges energy and equilibrates with the local tissue temperature.

Based on these assumptions, Pennes (1948) modeled blood effect as an isotropic heat source or sink which is proportional to blood flow rate and the difference between the body core temperature and local tissue temperature. Therefore, Pennes (1948) proposed a model to describe the effects of metabolism and blood perfusion on the energy balance within tissue. These two effects were incorporated into the standard thermal heat equation.

Consider a volume ( $V$ ) of the prostate with surface area ( $S$ ). By considering an elemental volume of mass  $dm = \rho dV$ , with  $\rho$  the density of the tissue, we can apply the conservation of energy to the inflow and outflow of heat across the control volume. The heat required to raise the temperature of the prostate from  $T_0$  to  $T$  is

$$dQ = \rho c dV (T - T_0) \quad (2.61)$$

where  $c$  is the heat required to raise the temperature of a unit mass of the prostate by 1K and  $T = T(x, y, z, t)$ . It thereby follows from 2.61 that

$$Q = \int \int \int \rho c dV (T_0 - T) \quad (2.62)$$

From the conservation of energy

$$\frac{dQ}{dt} = G - R \quad (2.63)$$

where  $G$  is the heat source given by

$$G = \int \int \int g dV \quad (2.64)$$

where  $g$  is the heat generated per unit time per unit volume. and  $R$  in equation 2.63 is heat outflow given by

$$R = \int \int \mathbf{q} \cdot d\mathbf{S} \quad (2.65)$$

with  $\mathbf{q}$  being the heatflow per unit area per unit time.

Using equations 2.62, 2.64 and 2.65 in equation 2.63, we get

$$\frac{d}{dt} \int \int \int dV \rho c (T - T_0) = \int \int \int dV g - \int \int \mathbf{q} \cdot d\mathbf{S} \quad (2.66)$$

Applying divergence theorem to the surface integral to make it a volume integral

$$\int \int \mathbf{q} \cdot d\mathbf{S} = \int_v \nabla \cdot \mathbf{q} dV \quad (2.67)$$

Substituting equation 2.67 into 2.66, and treating  $T_0$  as a constant of time. We get

$$\int_v dV \rho c \frac{\partial T}{\partial t} = \int_v g dV - \int_v (\nabla \cdot \mathbf{q}) dV \quad (2.68)$$

Re-arranging equation 2.68 and equating the integrands to zero for an arbitrary volume gives

$$\rho c \frac{\partial T}{\partial t} - g + \nabla \cdot \mathbf{q} = 0 \quad (2.69)$$

Since the Pennes equation is valid for isotropic systems, then we can apply the Fourier constitutive relation for  $\mathbf{q}$ .

$$\mathbf{q} = -k \nabla T$$

Then we can write equation 2.69 as

$$\rho c \frac{\partial T}{\partial t} - g - \nabla \cdot (k \nabla T) = 0 \quad (2.70)$$

Pennes treated the heat source as coming from the blood perfusion and heat due to body metabolism as given below

$$g = \rho_b c_b W_b (T_{ti} - T_{art}) - Q_m \quad (2.71)$$

Putting equation 2.71 into 2.70, we get the Pennes Bioheat equation used in this model.

$$\rho_{ti} C_{ti} \frac{\partial T}{\partial t} - \nabla \cdot (k \nabla T) - \rho_b c_b W_b (T_{art} - T_{ti}) - Q_m = 0 \quad (2.72)$$

where  $\rho_{ti}$ ,  $C_{ti}$ ,  $T_{ti}$  and  $k_{ti}$  are, respectively, the density, specific heat, temperature and thermal conductivity of tissue. Also,  $T_{art}$  is the temperature of arterial blood,  $Q_m$  is the metabolic heat generation and  $\rho_b$ ,  $c_b$  and  $W_b$  are, respectively, the density, specific heat and perfusion rate of blood.

The geometry used in this work contains both the spherically shaped prostate tissue and a spherically shaped transducer fused together. The focal region has a length of 2mm and a radius of 1mm while the prostate is spherical with a radius 10mm and height of 20mm as shown in fig. 3.1 below

The transducer is driven at a frequency of 1MHz. It is turned on for 1 second and then turned off to let the prostate tissue cool down under room temperature. The model thus solves for the heating of the tissue for 1s and then simulates the cooling process after the acoustic source is turned off.

The meshing used in any simulation alters the accuracy of the result. For a better accuracy, a finer mesh is required and as a recipe[23], the maximum mesh size to be used should not be greater than the wavelength of the sound wave which for the case of this simulation we determined from the source frequency using the basic sound relation.

$$\begin{aligned}c &= \lambda f \\ \lambda &= \frac{c}{f}\end{aligned}\tag{3.1}$$

Since in this modelling we have two different physics modules; the Partial Differential Equation module and the Bioheat Transfer module. Consequently, we shall create two meshes; one for the PDE and the other for the Bioheat Transfer. For the PDE simulation, the mesh resolve the wavelength of the source. The two different meshes are presented below

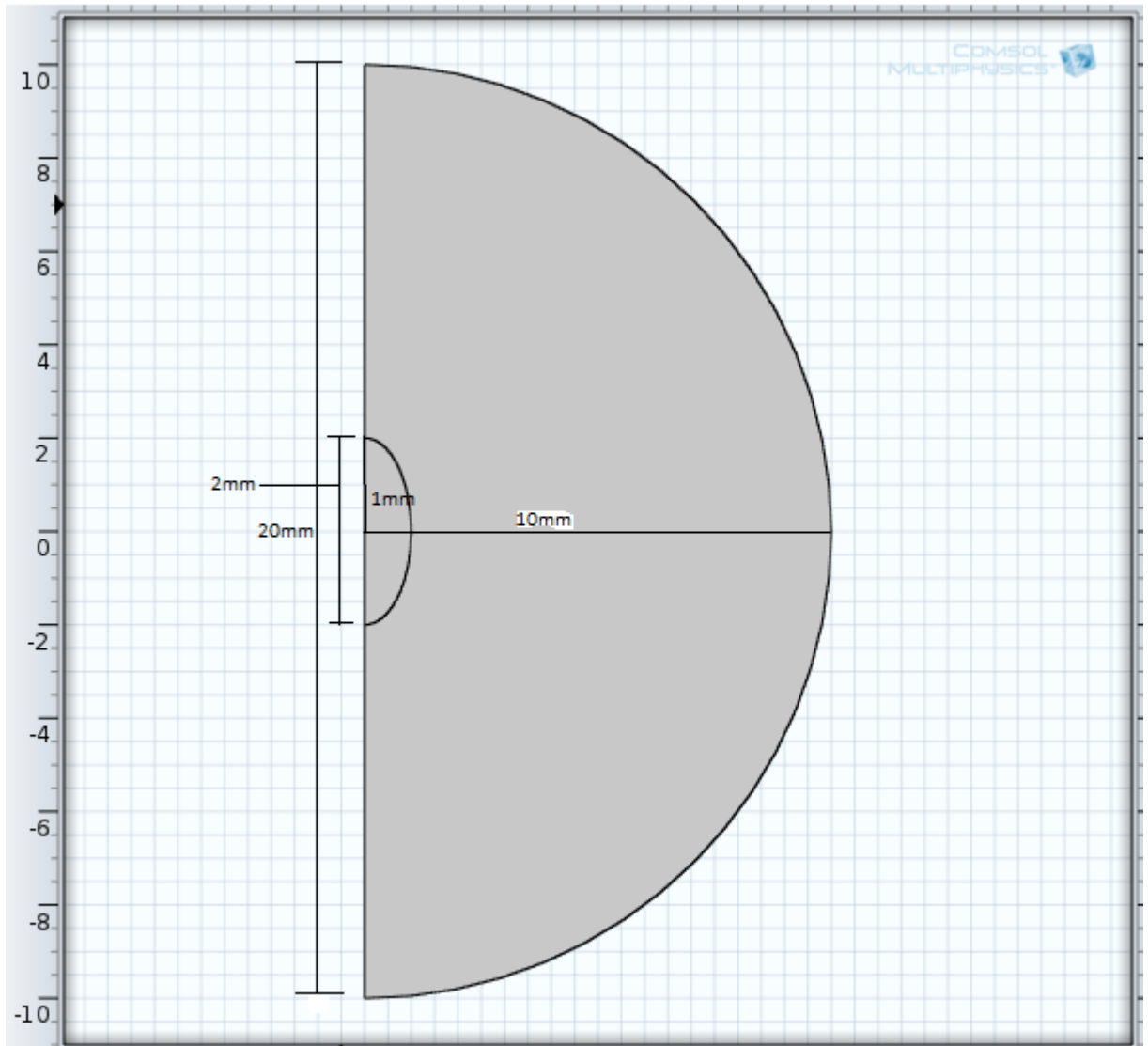


Figure 3.1: The Geometry; showing the prostate and the focal point both treated as a tissue domain.

### 3.1 Methodology

The model in this work uses the general form of Partial Differential Equation to simulate the transient sound wave as it passes through the tissue to the focal point where it converges. COMSOL uses Finite Element Analysis to discretize the prostate into 1282 elements as shown in figure 3.2. For each of this element, COMSOL solves the specified PDE to determine the pressure of each element. The pressure determined is inserted into equation 3.3 in order to obtain the heat source

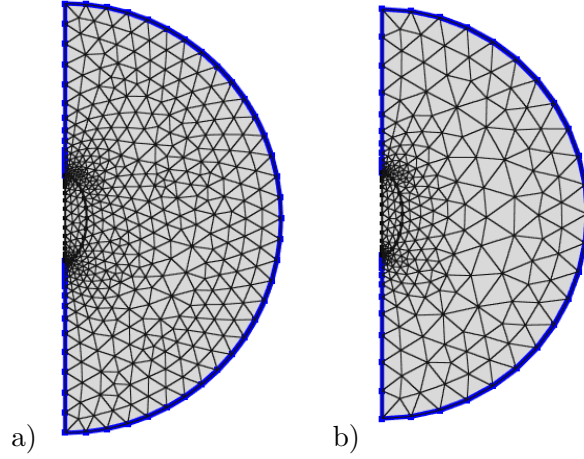


Figure 3.2: a) The figure of the mesh used for the PDE equation. b) The figure of the mesh used for the Bioheat Transfer

( $Q$ ) which is the heat generated by the PDE for the sound waves.

The heat source is also simulated by discretizing the prostate into 902 meshing elements and solving for each element the bioheat equation to find the heat distribution. Since the heat source which is in the focal region is much smaller than the size of the tissue, performing the simulation only in the tissue domain is a good approximation.

The partial differential equation is

$$e_a \frac{\partial^2 p}{\partial t^2} + d_a \frac{\partial p}{\partial t} + \nabla \cdot \Gamma = f \quad (3.2)$$

where

$$\Gamma = -\frac{\partial p}{\partial x} - \frac{\partial p}{\partial y}$$

and

$$f = -\frac{\delta}{c_0^4} \frac{\partial^3 p}{\partial t^3} - \frac{\beta}{\rho_0 c_0^4} \left( 2 \left( \frac{\partial p}{\partial t} \right)^2 + 2p \frac{\partial^2 p}{\partial t^2} \right)$$

Using the material properties given in reference [24] with the geometry described above, the equation above was solved to generate the pressure which is used to give the heat source  $Q$  given by

$$Q = \frac{2\alpha p^2}{\rho c_0} \quad (3.3)$$

where  $\alpha$  is the acoustic absorption coefficient,  $\rho$  is the tissue density and  $c$  the speed of sound in tissue. Using the Pennes' Bioheat Transfer equation to model heat transfer within the prostate tissue, the  $Q$  generated above is used as the heat source in the Bioheat equation. The parameters used in the current simulation are listed in the table below.

$$\rho_{ti} C_{ti} \frac{\partial T}{\partial t} - \nabla \cdot (k \nabla T) - \rho_b c_b W_b (T_{art} - T_{ti}) - Q_m = 0 \quad (3.4)$$



Table 3.1: A table of parameter values.

$c_0(m/s)$	$\rho_0(kg/m^3)$	$B/A$	$\alpha_0$	$y$
1500	1070	5	0.6	2

where  $T$  is the temperature,  $\rho_{ti}$ ,  $C_{ti}$ ,  $T_{ti}$  and  $k_{ti}$  are, respectively, the density, specific heat, temperature and thermal conductivity of tissue. Also,  $T_{art}$  is the temperature of arterial blood,  $Q_m$  is the metabolic heat generation and  $\rho_b$ ,  $C_b$  and  $W_b$  are, respectively, the density, specific heat and perfusion rate of blood. In this study, we assume that the properties of the prostate do not change under temperature rise, and also that the blood perfusion rate is negligible.

## 3.2 Boundary Condition

Boundary conditions are used to specify the nature of the boundaries of the computational environment in a way that best describes the physical problem. Some boundaries conditions define real physical obstacles like a sound wave bounced off by a rigid wall, or a moving interface. Other than acoustics, boundary conditions are applied to solve several physical problems. Boundary values or initial values are used in the solution of a set of differential equations arising from the physical problem. If the boundary gives a value to the normal derivative, then it is called Von Neumann boundary conditions while if the boundary gives a value to the problem, it is called Dirichlet Boundary Condition.

In a way to simulate the perturbation from the equilibrium state of the prostate tissue, a pulse of pressure source is applied with a step function that defunctionalizes the source after 1s. Since the prostate is initially at rest, suitable initial conditions are  $\frac{\partial P}{\partial t} = 0$  and  $P = 0$ , and at the boundaries of the prostate tissue, the boundary condition is set to 101.3KPa where 101.3KPa is the atmospheric pressure. For the Bioheat Transfer Physics, at a time  $t = 0$  before the sonication process, the prostate should be at normal body temperature.

## 3.3 PDE

There are two ways of using the mathematics module in COMSOL; either we use a readymade mathematics equation or we specify the equation that describes the physical problem under consideration. In this modelling, we did not use a readymade solution, rather we specified the exact equation from which was solved by COMSOL using Finite Element Analysis to give the pressure. There are three ways of specifying equations in COMSOL namely coefficient form, general form, and the weak form. In the coefficient form, the problem is specified through the setting of individual coefficients in a quite general system of partial differential equations and associated boundary conditions. The weak form is the most general and precise way of specifying the equations in a finite element context. In the general form, the equation is specified through the definition of a so called flux function in a conservation law formulation of the equation and it is this form that we use in this study.

The surface plot was made for both the pressure and temperature with and without the nonlinear term in the Westervelt wave equation at time  $t = 1s$  (see figure4.1 and figure4.3). The temperature surface plot indicates the concentration of the heat at the point of interest and it reduces radially outward which is as expected. The line graph which shows the increase in temperature with time is as shown below in figure4.2

It shows that the temperature rises within the first few seconds which is in accordance with literature [12] [25] [26]. Relating this with the surface plot, we may conclude that the tumor on the prostate tissue receives the maximum amount of heat and therefore may be destroyed if applied intermitently. The curve shows that after 1s, the temperature begins to equilibrate and consequently making the temperature rise reduce to zero. The surface plots of the pressure (figure4.3) and temperature (figure4.1)do not have much observable difference for both the Westervelt equation with and without the nonlinear term. They both indicate the concentration of energy at the location of the tumor.

The surface plot of the temperature after 10s as shown in figure4.1 shows that the temperature of the prostate has reduced significantly. This result is expected since the sonication is just for 1s and then allowed to cool down.

The pressure variation with time was taken at a point  $x = 8mm, y = 0$  away from the focal point (see figure 4.7) using the Westervelt equation for both cases when the nonlinear term is included and when it is not. The resulting graphs are presented in figure4.4. Both graphs indicate reduction in amplitude (attenuation) though one is more profound than the other. With the exclusion of the nonlinear term, the amplitude reduces from  $-1e-7Pa$  to about  $-8e-7Pa$ ; causing an attenuation of about  $-7e-7Pa$  while the attenuation increases to about  $-3.3e-7Pa$  when the nonlinear term is included.

This conclusively means that an additional attenuation of about  $-4e-7Pa$  is caused by the nonlinear term. On the time scale used in this modelling, this is a significant difference.

With the omission of both the third order derivative and the nonlinear term the amplitude of the

attenuated node is about  $-2.5 \times 10^{-6} \text{Pa}$  as shown in figure 4.5, which is the least attenuated among them all.

This study agrees with the work of Jafarian et al [12] and the in-vivo experiment in that the rate of temperature rise is very sharp at the beginning of the sonication and starts to decline after the source is turned off making the curve approach equilibrium as indicated in figure 4.2.

Curiel et al [25] performed an experiment on the evaluation of lesions prediction modeling in the presence of ultrasound waves. In the experiment, they observed that the temperature rises steeply during the first few seconds of sonication. This agrees with the graph above. In another work done by Souchon et al [26], it was predicted that a steep temperature gradient may occur during the sonication of a liver sample.

## 4.1 Conclusion

Due to the high energy transfer of ultrasound wave, HIFU is becoming a popular method of cancer treatment. However, in some specific cases such as the cancer of the liver [11], the method is obdurately applied. In this study, since the attenuation due to the nonlinear term is negligible (order of  $10^{-7} \text{Pa}$ ), then it is safe to treat the Westervelt equation without the consideration of the nonlinearity of the medium. Also from the temperature rise against time which is same for the three processes, it is safe to conclude that acoustic streaming and convective cooling are negligible since the prostate has no significantly large blood vessel.

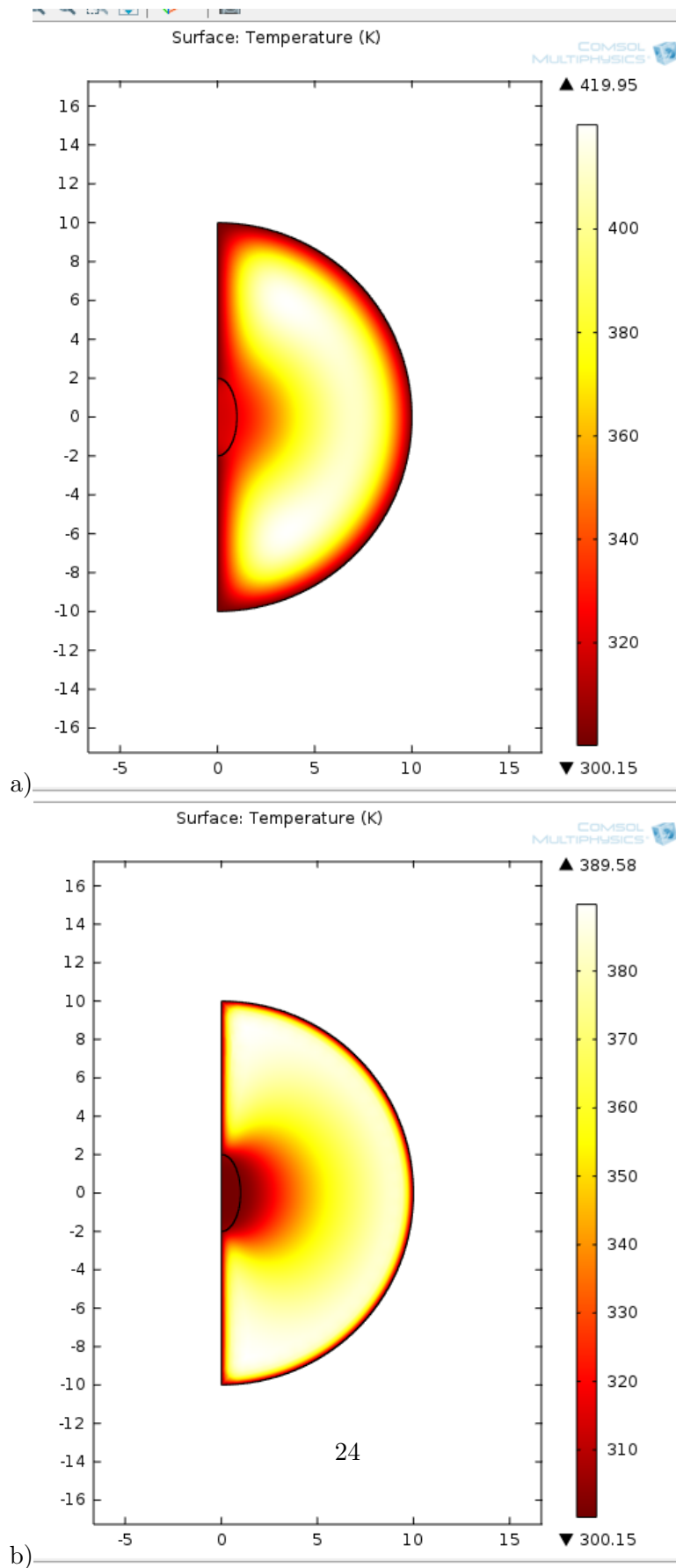


Figure 4.1: a) Surface Plot of Temperature at time  $t=1s$ . b) Surface Plot of Temperature at time  $t=10s$

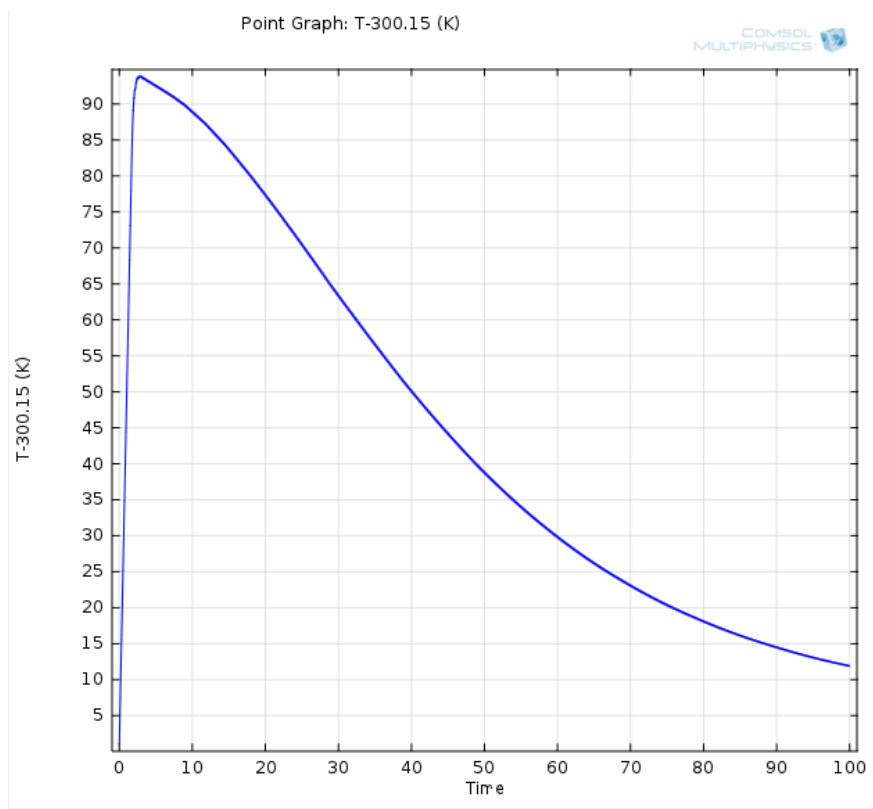
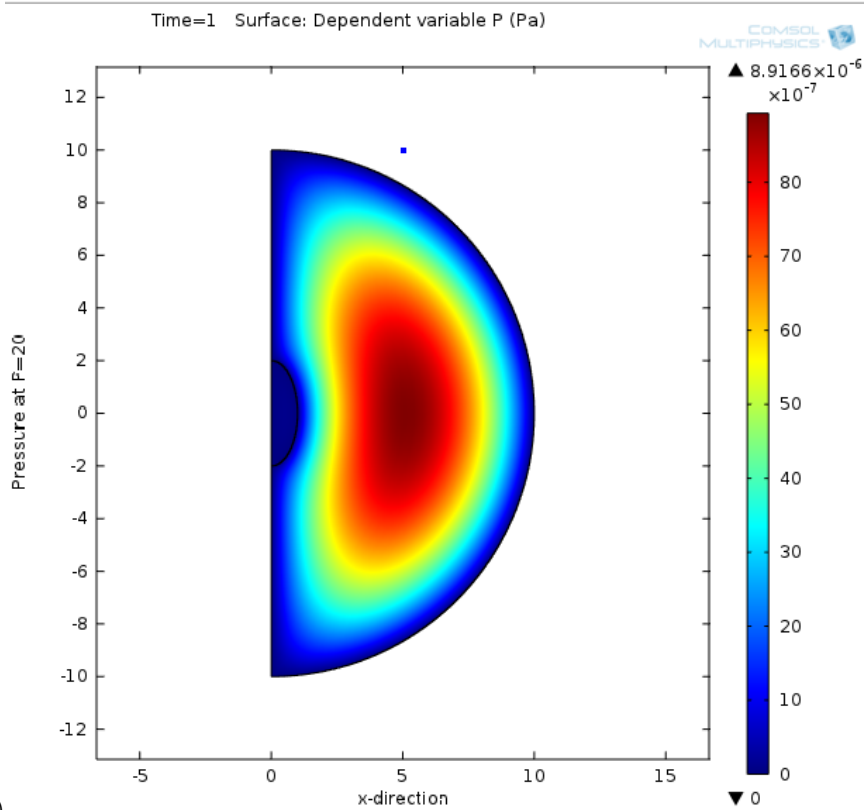
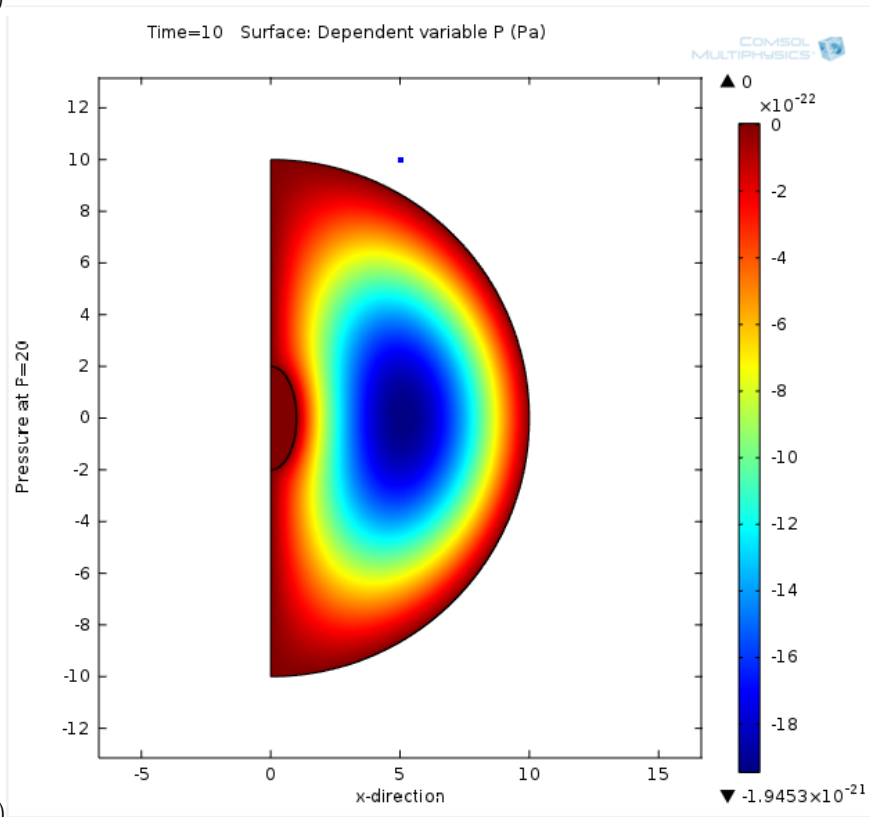


Figure 4.2: a) A line plot of the temperature variation with time.



a)



b)

Figure 4.3: a) Surface Plot of pressure at time  $t=1s$ . b) Surface Plot of pressure at time  $t=10s$

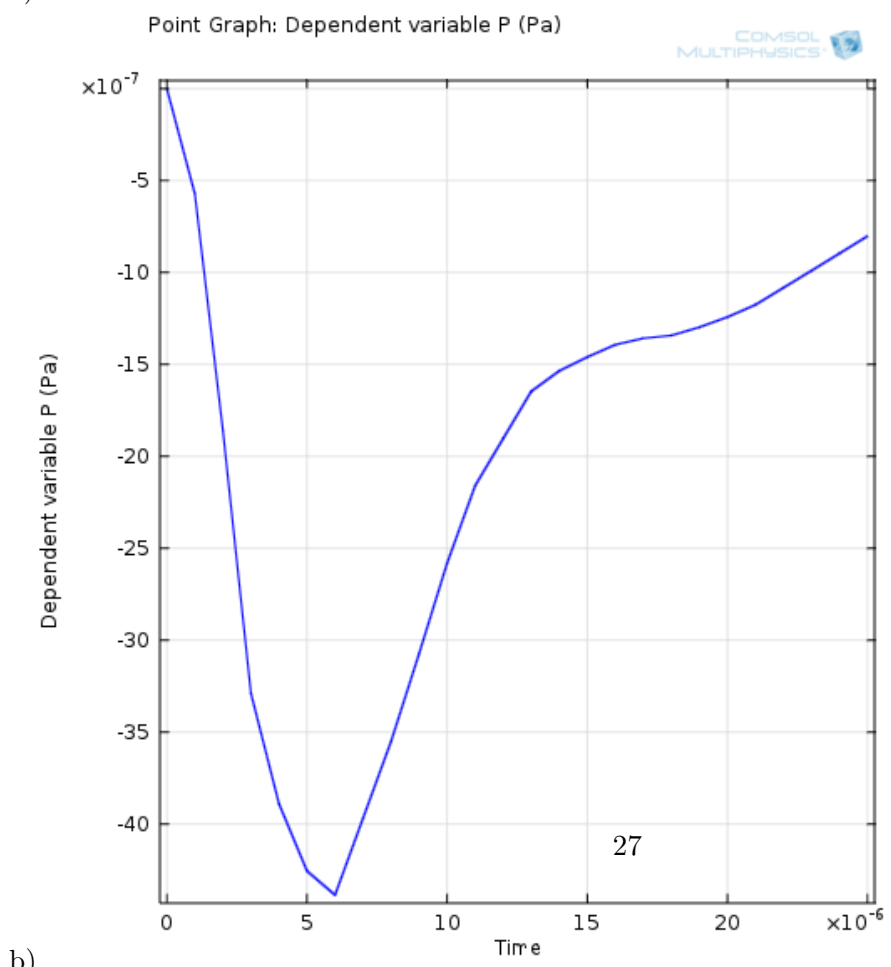
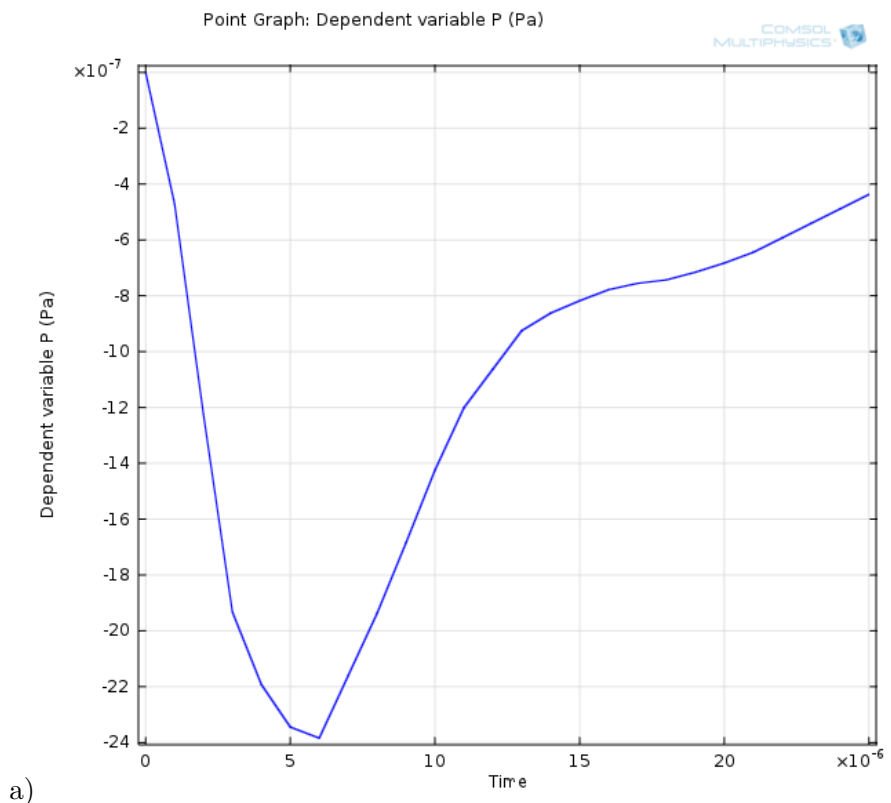


Figure 4.4: a) A line graph of the pressure variation with time when the nonlinear term is included. b) Line plot for the pressure variation with time using the Westervelt up to the third order and neglecting the nonlinear term

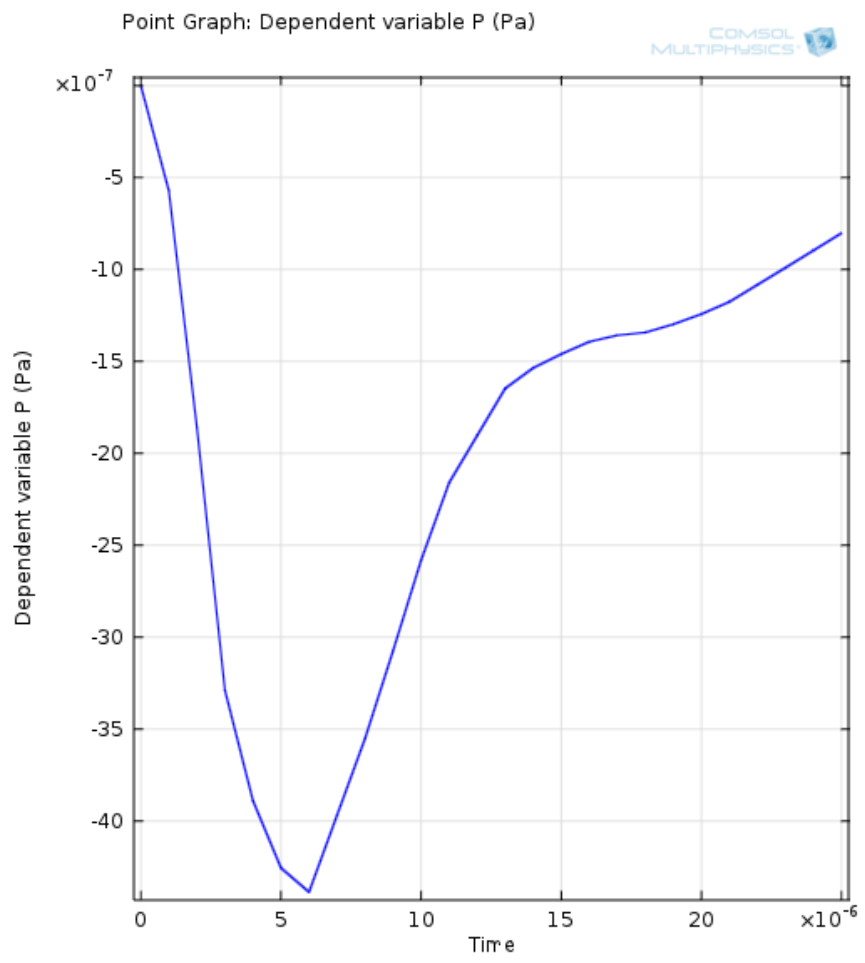


Figure 4.5:



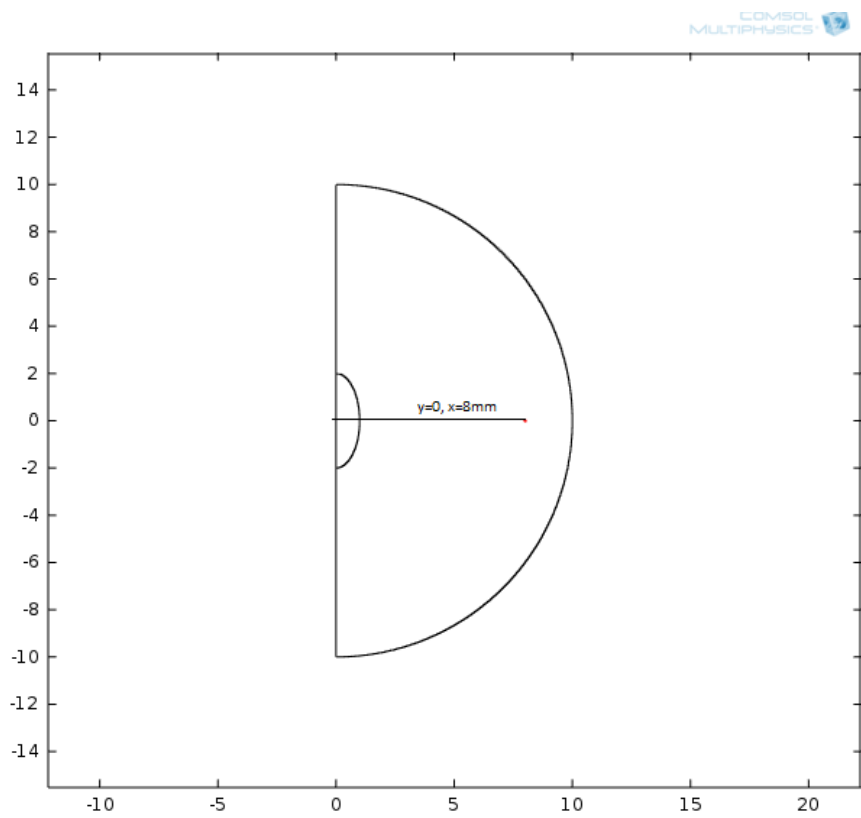


Figure 4.6: The point indicate the position whose pressure is plot against time

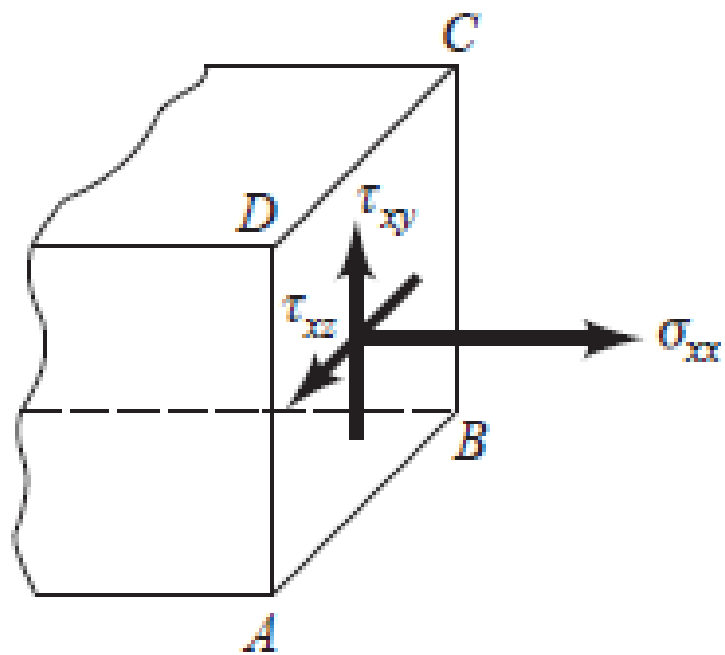


Figure 4.7: A figure showing the action of both shear and normal stresses acting on a body of fluid

- [1] L.D Landau and E.M Lifshit.  
*Fluid Dynamics, 2nd Edition. Institute of physical problems, U.S.S.R Academy of Sciences. Vol 6 of course of Theoretical Physics.*
- [2] F.A Duck.  
*Physical Properties of Material, .*
- [3] W. Chen, S. Holm  
“ *Fractional laplacian time-spaced models for linear and nonlinear lossy media*”,
- [4] A. Rozanova Pierrat. *Derivation and validation of the Khokhlov-Zabolotskaya-Kuznestov (KZK) equation for viscous and non-viscous thermoelastic media*, A Comprehensive Refer
- [5] T. Leissing, P. Jean, J. Defrance, C. Soize  
“*Nonlinear parabolic equation model for finite amplitude sound propagation over porous ground layers*“,
- [6] Fabrice and Sverre (2011) *Nonlinear Acoustic wave equations with fractional loss operator*,
- [7] Pedro Moreira, Igor Peterlik et al(2013) *Modelling Prostate Deformation: SOFA Vs Experiment*, doi:10.5539/mer.v3n2p64
- [8] L.D Landau and E.M Lifshit  
*Fundamentals of Fluid Dynamics.*
- [9] N.T. Sanghvi, K.Hynynan, and F.L Lizzi  
‘ *New developments in therapeutic ultrasound*’ *IEE Eng.Med.Bio. Mag. Vol.15, no.6, pp 83-92, 1996,*
- [10] Jun-Yuan Jeng et al.  
*Exposed criteria for medical diagnostic ultrasound: II criteria based on all known mechanism*’

*Diagnostic ultrasound safety; A summary technical report. issued by the National Council on Radiation Protection and Measurements,*

- [11] Solovchuk, Tony, Sheu, Marc, et al  
*Image-Based computational model using focused ultrasound ablation of liver tumor* .  
dx.doi.org/10.1021/jz500113x — J. Phys. Chem. Lett. 2014, 5, 1511–1515.
- [12] F. Jafarian Ali Shakhari-zadeh, S.khoei et al.  
*Thermal Distribution of ultrasound waves in prostate tumor: Comparison of computational modelling with vivo experiment* , Photonics for Solar Energy Systems V, Andreas Gombert, Proc. of SPIE Vol. 9140, 91400Y · © 2014 SPIE, doi: 10.1117/12.2052375
- [13] S.W. Kenstra and A Hirschberg *An Introduction to Acoustics* ,
- [14] A.D Pierce
- [15] Medical News Today (MNT), Article 150086 *Acoustics: An Introduction to its physical principal and application* . Mc. Graw -HIU Book company. Inc. New York 1981. Also available from the acoustic society of America
- [16] C.Cattaneo (1958), "Sur une forme de lequation de la chouler eliminant le parado.
- [17] P. Vernotte  
*"Les paradoxes de la theorie continue de l'equation de la chaleur (Paradoxes in the continuous theory of the heat equation)," C.R. Acad. Sci. 246, 3154–3155(1958).*
- [18] Hwang Steve and Ellen Arruda.  
*Mechanical Characterization of Human Prostate (2013),*
- [19] M. Gurtin and A. Pipkin.  
*A general theory of heat with finite wave speeds* Arch.Ration.Mech.Anal.31, 113-126,(1968)
- [20] Fabrice and Sverre  
*Nonlinear Acoustic wave equations with fractional loss* , Acoustic Society of America
- [21] Chandra Sekharaiah,  
*Thermoelasticity with second sound: A review.* Appl. Mech. Rev 39, 705-729
- [22] Hamilton and Morfey  
*M. F. Hamilton and C. L. Morfey,*. "Model equations," in *Nonlinear Acoustics*, edited by M. F. Hamilton and D. T. Blackstock (Academic Press, San Diego, 1998), Chap. 3, pp. 41–63.
- [23] COMSOL Manual,  
*Introduction to Acoustic Module*

- [24] Forough Jafarian, Ali Shakeri-Zadeh, Samideh Khoei et al,  
*Thermal distribution of Ultrasound waves in Prostate tumor; Comparison of computational modelling with In Vivo Experiment'* Hindawi Publishing Corporation. *ISRN Biomathematics*.
- [25] L. Curiel, E.R.Feno et al,  
*Medical Imaging Physics, Ch. 19, Wiley, New York, NX, U.S.A, 4th Edition (2002)*
- [26] R. Souchon, G.Bouchoux, E. Maciejko et al,  
*"Monitoring the formation of thermal leison with heat-induced echo-strain imaging: a feasibility study," Ultrasound in Medicine and Biology, vol 31, no.2, pp251-259,(2005)*